



Description of a Rare Pyomelanin-Producing Carbapenem-Resistant *Acinetobacter baumannii* Strain Coharboring Chromosomal OXA-23 and NDM-1

Feng Zhao,^{a,b} Haiyang Liu,^{c,d,e} Yue Yao,^{c,d,e} Linghong Zhang,^{c,d,e} Zhihui Zhou,^{c,d,e}  Sebastian Leptihn,^{c,f,g}
 Yunsong Yu,^{c,d,e}  Xiaoting Hua,^{c,d,e}  Ying Fu^{a,b}

^aDepartment of Clinical Laboratory, Sir Run Shaw Hospital, Zhejiang University School of Medicine, Hangzhou, Zhejiang, China

^bKey Laboratory of Precision Medicine in Diagnosis and Monitoring Research of Zhejiang Province, Hangzhou, Zhejiang Province, China

^cDepartment of Infectious Diseases, Sir Run Shaw Hospital, Zhejiang University School of Medicine, Hangzhou, Zhejiang, China

^dKey Laboratory of Microbial Technology and Bioinformatics of Zhejiang Province, Hangzhou, Zhejiang, China

^eRegional Medical Center for National Institute of Respiratory Diseases, Sir Run Run Shaw Hospital, Zhejiang University School of Medicine, Hangzhou, Zhejiang, China

^fZhejiang University-University of Edinburgh (ZJU-UoE) Institute, Zhejiang University, International Campus, Haining, Zhejiang, China

^gCollege of Medicine & Veterinary Medicine, University of Edinburgh Medical School, Edinburgh, United Kingdom

Feng Zhao and Haiyang Liu contributed equally to this article. The author order was determined by seniority.

ABSTRACT Carbapenem-resistant *Acinetobacter baumannii* (CRAB), which belonged to global clones 1 (GC1) or 2 (GC2), has been widely reported and become a global threat. However, non-GC1 and non-GC2 CRAB strains are not well-studied, especially for those with rare phenotype. Here, one pyomelanin-producing CRAB strain (*A. baumannii* DETAB-R21) was isolated from oral swab in the ICU. Antimicrobial susceptibility testing showed it was resistant to carbapenems, ceftazidime, levofloxacin, and ciprofloxacin. DETAB-R21 was ST164_{Pas} and ST1418_{Oxf} with KL47 and OCL5, respectively. Whole-genome sequencing (WGS) analysis revealed chromosome contained three copies of *bla*_{OXA-23} on three 4,805-bp Tn2006 composite transposons with various novel 9-bp target site duplications (TSD). A Tn125-like structure, including *bla*_{NDM-1}, a novel 4,343 bp composite transposon encoding *bla*_{CARB-16}, and three prophage regions were also identified. Importantly, *hmgA* was interrupted by a Tn2006 and contributed to pyomelanin production and further confirmed by *hmgA* overexpression. Furthermore, *A. baumannii* irradiated with UV light, DETAB-R21 showed a higher relatively survival rate compared to a control strain that did not produce pyomelanin. No effects of pyomelanin were observed on disinfectants susceptibility, growth, or virulence. In conclusion, pyomelanin-producing CRAB carrying the *bla*_{NDM-1} and *bla*_{OXA-23} genes embedded in the bacterial chromosome is of grave concern for health care settings, highlighting the need for effective measures to prevent further dissemination.

IMPORTANCE Pyomelanin production is a quite rare phenotype in *A. baumannii*. Moreover, the mechanisms leading to the pyomelanin production was still unclear. Here, we for the first time, confirmed the mechanism of pyomelanin production, and further investigated the impact of pyomelanin on disinfectants susceptibility, growth, virulence, and UV irradiation. More importantly, many mobile genetic elements (MGEs), including three copies of Tn2006 composite transposons, one copy of *bla*_{NDM-1} on the Tn125-like structure and three prophage regions, were identified in the chromosome, demonstrated strong plasticity of *A. baumannii* genome. Our study provides important insights into the new rare ST164_{Pas} *A. baumannii* strain with high level carbapenem resistance, which is of great threat for patients. These findings will provide important insights into the resistance gene transfer via transposition events and further spread in the clinic.

KEYWORDS CRAB, pyomelanin, *hmgA* overexpression, Tn2006, Tn125-like transposon

Editor Xiaoyu Tang, Shenzhen Bay Laboratory

Copyright © 2022 Zhao et al. This is an open-access article distributed under the terms of the [Creative Commons Attribution 4.0 International license](https://creativecommons.org/licenses/by/4.0/).

Address correspondence to Xiaoting Hua, xiaotinghua@zju.edu.cn, or Ying Fu, ying.fu@zju.edu.cn.

The authors declare no conflict of interest.

Received 7 June 2022

Accepted 24 July 2022

Published 10 August 2022

A *Acinetobacter baumannii* is a major cause of nosocomial infections affecting mainly patients in the intensive care unit (1). Importantly, in 2019, Centers for Disease Control and Prevention (CDC) report carbapenem-resistant *Acinetobacter* as “Urgent Threats” (2). Nosocomial outbreaks causing carbapenem-resistant *A. baumannii* (CRAB) strains are emerging rapidly worldwide and pose a huge threat to global health (3), particularly due to the increasing frequency of multidrug resistant (MDR) infections (4).

Most CRAB infections are caused by strains that belong to global clones 1 (GC1) or 2 (GC2), with GC2 accounting for the vast majority of sequenced carbapenem-resistant isolates (5). However, non-GC1 and non-GC2 CRAB strains, such as ST164_{Pasr} are reported rarely. As well documented, OXA-23, the class D β -lactamase to be identified from CRAB, still remains the most common contributor to carbapenem resistance (6). The *bla*_{OXA-23} gene is most frequently located in Tn2006, Tn2008 or Tn2009 transposons flanked by the insertion sequence *ISAbA1* and was widely reported (7). However, some metallo- β -lactamase genes (*bla*_{NDM}, *bla*_{VIM}, and *bla*_{IMP}) are relatively rare in *A. baumannii* but are occasionally found in the bacterial chromosome or in plasmids (5, 8). The *bla*_{NDM-1} gene is commonly located in the Tn125 transposon (9). However, no studies have reported the existence of *bla*_{OXA-23} and *bla*_{NDM-1} in the chromosome of *A. baumannii* at the same time.

Pigmentation of clinical strains of CRAB has rarely been observed. The presence of a reddish-brown pigment, pyomelanin, causes a quite rare phenotype, reported only twice (10, 11). The overproduction of the pyomelanin is caused due to changes in the tyrosine metabolic pathway and is based on the deletion of the *hmgA* encoding homogentisate dioxygenase (HmgA) by *ISAbA1* (11). Pyomelanin-producing *A. baumannii* can show resistance to a wide range of antimicrobial drugs (11), which in turn could become a new challenge in the clinical setting, especially in the ICU.

Here, we characterize the genome of a rare pyomelanin-producing CRAB (DETAB-R21) collected from the oral swab from patient in the ICU, which carries three copies of *bla*_{OXA-23} in Tn2006 and one copy of *bla*_{NDM-1} in Tn125-like composite transposons in the chromosome. To our knowledge, we confirmed the mechanism of pyomelanin generation for the first time while also investigating the fitness cost, virulence, and UV resistance of the pyomelanin-producing CRAB isolate.

RESULTS

Genome analysis of the clinical strain *A. baumannii* DETAB-R21. The complete genome of *A. baumannii* DETAB-R21 was obtained from a hybrid assembly of Illumina and Nanopore (MinION) reads sequencing data. In addition to a chromosome of a size of 3,862,196 bp, the strain contains five plasmids (Table 1). The chromosome has an overall GC content of 39% (Table 1) and contains 20 XerC/XerD (C/D) and XerD/XerC (D/C) recombinases recognition sites (Fig. S1). Based on the Pasteur and Oxford MLST schemes, DETAB-R21 is ST164_{Pas} (*cpn60-40*, *fusA-3*, *gltA-7*, *pyrG-2*, *recA-40*, *rplB-4*, *rpoB-4*) and ST1418_{Oxf} (*cpn60-36*, *gdhB-58*, *gltA-21*, *gpi-114*, *gyrB-48*, *recA-42*, *rpoD-4*). Both MLST schemes of XH1935 are identical to DETAB-R21, with only a 5-bp difference in their genome based on the SNP analysis.

The software *Bautype* showed DETAB-R21 contains OC locus 5 (OCL-5), matching the reference sequence with 99.64% nucleotide identity. The K locus in DETAB-R21 is KL47, to which it matches 100% of the locus with an overall nucleotide identity of 96.89%. Similarly, the software *Kaptive* revealed identical KL and OCL types.

ResFinder detected nine antibiotic resistance genes in the DETAB-R21 genome (Table 1). All resistance genes are in the chromosome (Table 1). Two of these, *bla*_{ADC-52} and *bla*_{OXA-91} represent the native AmpC and OXA-51 β -lactamase genes. Additionally, one Tn6168 carried *bla*_{ADC-176} is located in the chromosome with 11-bp target site duplications (TSD) (Fig. 1a). Moreover, there are three copies of *bla*_{OXA-23} on the 4,805-bp Tn2006 composite transposon structure with the different sequence of the 9-bp TSD on either side and one copy of *bla*_{NDM-1} and *ble*_{MBL} on the Tn125-like structure flanked by 5-bp TSD (AAGTT) mediated by *ISAbA125* (Fig. 1b). Two copies of *ISAbA14* transposons were also observed flanked by three possible TSD (TAT). The Tn125-like of DETAB-R21 has a 99.99% identity compared to the transposon in *A. baumannii* TP2 (GenBank accession [CP060011](https://www.ncbi.nlm.nih.gov/nuccore/CP060011)), collected from clinical sample

TABLE 1 Characteristics of DETAB-R21 genome components

Element	Replicon type	Size (bp)	GC content	Antibiotic resistance genes
Chromosome		3,862,196	38.97%	<i>bla</i> _{ADC-52r} , <i>bla</i> _{ADC-176r} , <i>bla</i> _{OXA-91r} , <i>bla</i> _{OXA-23r} , <i>bla</i> _{NDM-1r} , <i>ble</i> _{MBLr} , <i>bla</i> _{CARB-16r} , <i>aph</i> (3')-VI, <i>ant</i> (3')-IIa
pDETABR21-1		12,709	32.94%	
pDETABR21-2		4,554	41.26%	
pDETABR21-3		2,924	37.82%	
pDETABR21-4	Aci1	2,742	37.24%	
pDETABR21-5	Aci4	2,309	38.54%	

in USA in 2020 (Fig. 1b). Moreover, Tn125-like structure in *A. baumannii* ACN21 (GenBank accession CP038644), which is isolated from a blood sample in India in 2019, is also identical to that of DETAB-R21 with a percentage of 99.93%. In addition, a novel 4,343 bp ISAb1 composite transposon containing *bla*_{CARB-16} was also identified in the chromosome. Moreover, there was an amino acid mutation of *gyrA* (S81L), which could confer resistance to fluoroquinolones.

Genetic analysis of plasmids contained in strain DETAB-R21. We identified five plasmids in DETAB-R21, namely, pDETABR21-1 to pDETABR21-5, with sizes between 2,309-bp to 12,709-bp and GC contents ranging from 37% to 39%. None of the plasmids carried resistance genes (Table 1). Based on an analysis of the replicons, pDETABR21-4 and pDETABR21-5 carry the *repAci1* and *repAci4* replication genes, respectively (Table 1). The remaining three plasmids contain so far undescribed replicons.

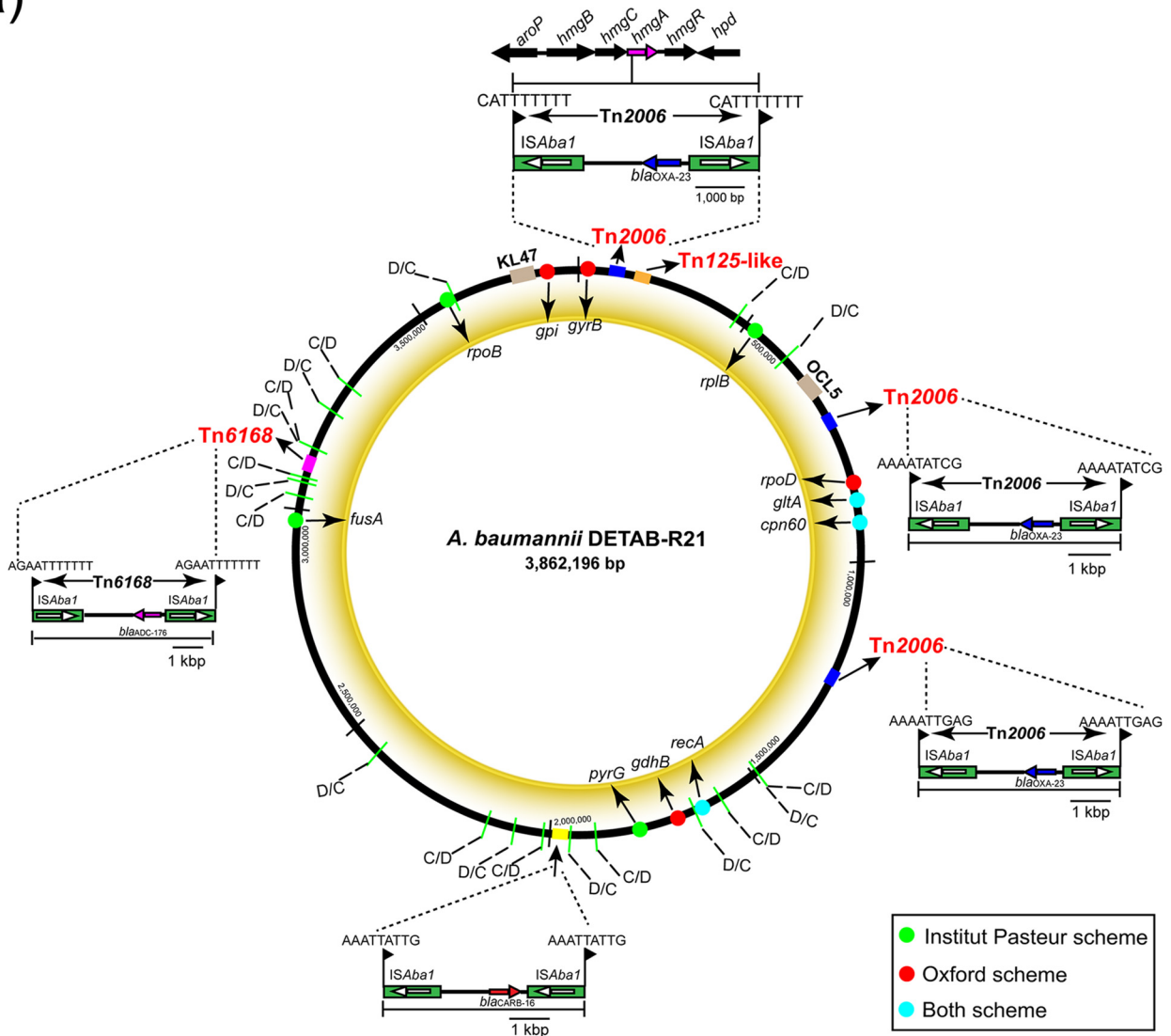
Prophage regions in the chromosome. Prophages play an important role in the biology of bacteria and can contribute to virulence of bacteria (12). Application of the tool PHASTER to predict the prophage regions, showed two prophages that are considered “intact” meaning they are likely able to undergo replication (Φ DETAB-R21-I, from 1,266,431-bp to 1,303,890-bp; Φ DETAB-R21-III, from 3,150,251-bp to 3,174,492-bp). In addition, one questionable prophage region was identified (Φ DETAB-R21-II, from 2,567,218-bp to 2,618,277-bp) which might potentially not be able to form phage progeny (Fig. 2). Φ DETAB-R21-I, Φ DETAB-R21-II and Φ DETAB-R21-III have a length of 37.4 kb, 51 kb and 24.2 kb with the GC content of 40.62%, 38.28% and 40.61%, respectively. Moreover, prophage Φ DETAB-R21-I and Φ DETAB-R21-II regions are both flanked by 16-bp and 21-bp attachment (*att*) sites, namely, *attL* and *attR*, respectively (Fig. 2). Based on the PHASTER tool, prophage Φ DETAB-R21-I was predicted to be intact due to the score of 110, whereas Φ DETAB-R21-II (score, 90) was classified as questionable while also flanked by the *attL* and *attR* sites. Although no *attL* and *attR* sites were found in Φ DETAB-R21-III, the putative prophage has a high score (150) and was identified as intact.

***hmgA* plays a key role in pyomelanin production.** The wild-type strain DETAB-R21 produced a pigment on MH agar plates, which we later identified as pyomelanin (Fig. 3). In contrast, XH1935 displays the usually observed phenotype with pale white colonies (data not shown). To explore the molecular basis of pigment production, we investigated the key genes in the pathway of pigment production. Results revealed that *hmgA* was interrupted by a Tn2006 with 11-bp TSD (CATTTTTT) (Fig. 1a). We then introduced a plasmid into the strain, leading to *hmgA* overexpression (DETAB-R21 + pYMAb2:pompA:*hmgA*). Here, we observe that pigment production was abolished, leading to the normally observed phenotype (Fig. 3). The control, a complementation with a pYMAb2-Hyg^r empty vector, showed pigment production similar to the strain without any plasmid, producing pyomelanin at similar levels (Fig. 3).

Antimicrobial agents and disinfectants susceptibility profiles. The results of AST showed that DETAB-R21 is resistant to imipenem (128 mg/L), meropenem (256 mg/L), ceftazidime (>256 mg/L), levofloxacin (8 mg/L), and ciprofloxacin (8 mg/L) but still remained susceptible to gentamicin (2 mg/L), tobramycin (0.5 mg/L), colistin (0.125 mg/L), and tigecycline (2 mg/L) (Table 2). Moreover, DETAB-R21 + pYMAb2:pompA:*hmgA*, DETAB-R21 + pYMAb2 and XH1935 presented the same antimicrobial susceptibilities compared with DETAB-R21-WT. The MICs for three kinds of disinfectants showed that all stains have the same pattern of susceptibility.

Growth ability and virulence comparison. Growth dynamics were measured as a proxy for fitness in order to compare the bacterial propagation of strains that produce pyomelanin to those that do not. However, no observable differences were detected when

(a)



(b)

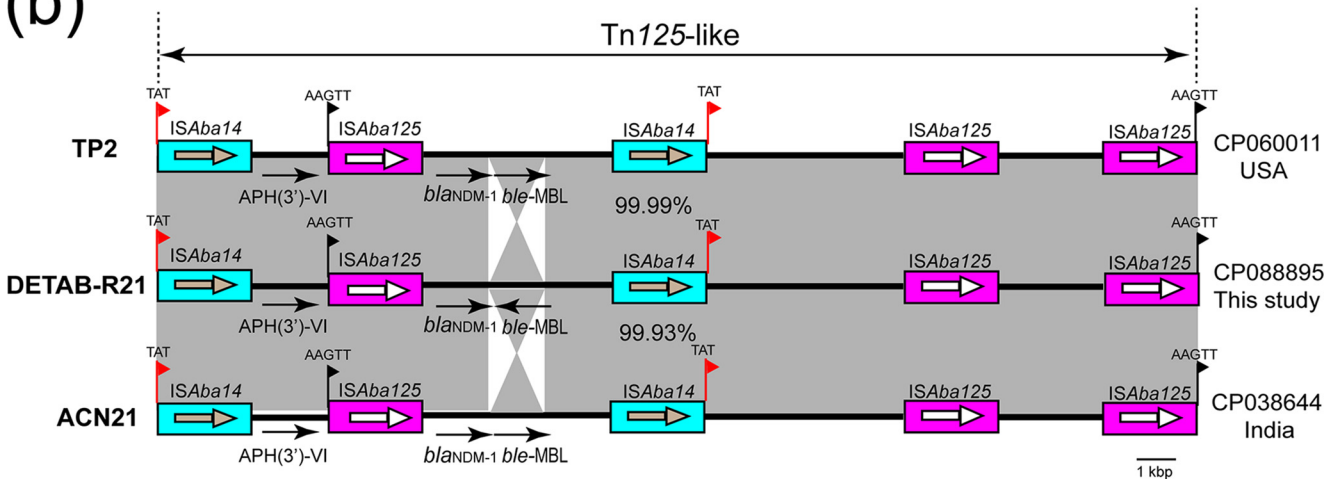


FIG 1 *A. baumannii* DETAB-R21 chromosome and transposons structure. (a) Circular map of the *A. baumannii* DETAB-R21 chromosome. Housekeeping genes used in MLST schemes are indicated by various colors. The structure of Tn2006 is shown as blue filled box. *hmgA* was interrupted by one copy of (Continued on next page)

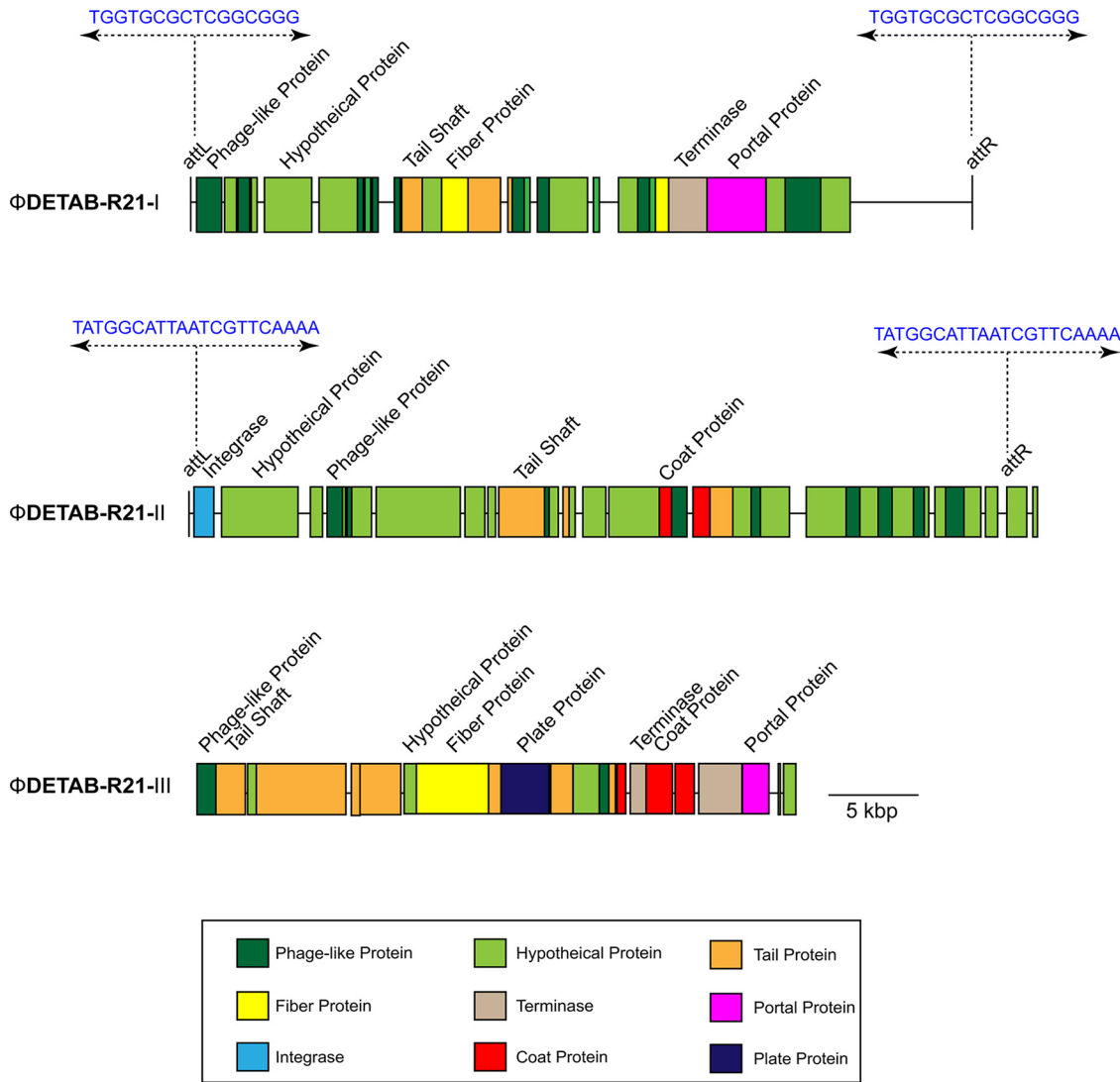


FIG 2 Predicted prophage regions within the *A. baumannii* DETAB-R21 chromosome. The length of ΦDETAB-R21-I, ΦDETAB-R21-II and ΦDETAB-R21-III are 37.4 kb, 51 kb and 24.2 kb, respectively. attL and attR are shown as blue bases at both ends of ΦDETAB-R21-I and ΦDETAB-R21-II. Genes are color-coded based on predicted functions.

comparing the wild type DETAB-R21, with or without plasmid-mediated *hmgA* overexpression (or the empty control vector) and strain XH1935 (Fig. 4a).

Next, we determined if pyomelanin influences the virulence of *A. baumannii*. To this end, the *in vivo* model *G. mellonella* was used. Half of the larvae died after 12 h postinjection in the case of the virulent strain *A. baumannii* AB5075 (Fig. 4b). All pyomelanin producing and no pyomelanin producing *A. baumannii* strains were less virulent compared to *A. baumannii* AB5075 ($P < 0.0001$). More importantly, no differences were observed regarding the virulence of pyomelanin-producing DETAB-R21-WT and no pyomelanin producing strain XH1935 ($P = 0.1653$). We also did not observe any statistical difference for DETAB-R21-WT and DETAB-R21 + pYMAb2:pompA:*hmgA* ($P = 0.2011$). The survival rates of DETAB-R21-WT, plasmid-complemented strains leading to *hmgA* overexpression or containing the empty

FIG 1 Legend (Continued)

Tn2006. Tn125-like is shown as orange filled boxes. Tn6168 is shown as red violet filled box. The novel transposon of *bla*_{CARB} is shown as yellow filled box. Short black lines represent the *pdif* sites, with the orientations of XerC (C) and XerD (D). Target site duplications (TSD) shown on either side of the transposons are indicated using black flags. (b) Structure of Tn125-like compared with *A. baumannii* TP2 (CP060011) and *A. baumannii* ACN21 (CP038644). Horizontal arrows represent the direction of genes, with black arrows indicating resistance genes. Light blue filled boxes indicate ISAb14 copies. Red violet filled boxes indicate ISAb125 copies. Gray shades indicate regions with 99.9%–100% identity. TSD is shown as flag using red or black.

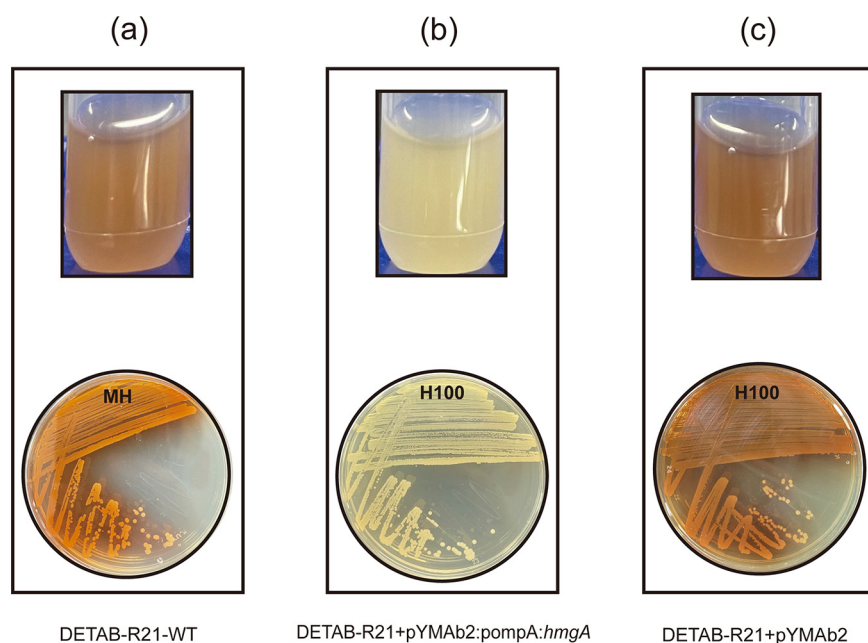


FIG 3 Pyomelanin generation of *A. baumannii* strains on MH agar plates and MH broth with or without hygromycin. (a) DETAB-R21-WT could produce pyomelanin on both media without hygromycin. (b) *hmgA* overexpression strains DETAB-R21+pYMAb2:pompA:*hmgA* failed to produce pigment. (c) DETAB-R21+pYMAb2 is an empty vector strain without hygromycin production in the presence of hygromycin.

control vector, and XH1935 strains were all highly similar to each other in the *G. mellonella* model (Fig. 4b).

Bacterial survival rates under UV irradiation. As pigments have the ability to absorb light and protect light sensitive molecules such as DNA, we tested if the pigmented strain is less sensitive to UV radiation with three independent assays. Indeed, DETAB-R21-WT displayed a higher relative survival rate compared to XH1935 when exposed to 20 s (about 75% VS 35%) and 40 s (35% VS 10%) (Fig. 5). When pigment production was suppressed by introducing the wild-type gene on a plasmid, similar survival rates were observed in DETAB-R21+pYMAb2:pompA:*hmgA* and XH1935 (Fig. 5). All strains did not survive prolonged UV irradiation for 60 s or longer.

DISCUSSION

Emergence and spread of multidrug resistant (MDR) *A. baumannii* are growing clinical problems throughout the world, posing a threat to public health (13, 14). This species has become one of the most important nosocomial pathogens that easily adapts to the hospital environment, particularly in the intensive care unit (ICU), and is able to disseminate rapidly in the environment and patients (15). Here, we have described the complete genome sequence of a rare pyomelanin-producing CRAB DETAB-R21, a ST164_{pas} and ST1418_{oxf} strain collected from an ICU patient. Previous reports have shown that resistance to carbapenems is usually mediated by OXA-23, OXA-24 and OXA-58 in *A. baumannii* (16). Coharboring of

TABLE 2 MICs of antibiotics against DETAB-R21

Isolates	Antibiotic ^a minimum inhibitory concn (mg/L) ^b									Disinfectants ^c (mg/L)		
	IMP	MEM	CAZ	GEN	TOB	LEV	CIP	COL	TGC	CHG	p-CP	Ca(OCl) ₂
DETAB-R21-WT	128 (R)	256 (R)	>256 (R)	2 (S)	0.5 (S)	8 (R)	8 (R)	0.125 (S)	2 (S)	4	256	>2048
DETAB-R21+ pYMAb2:pompA: <i>hmgA</i>	128 (R)	256 (R)	>256 (R)	2 (S)	1 (S)	8 (R)	8 (R)	0.125 (S)	2 (S)	4	256	>2048
DETAB-R21+pYMAb2	128 (R)	256 (R)	>256 (R)	2 (S)	1 (S)	8 (R)	8 (R)	0.125 (S)	2 (S)	4	256	>2048
XH1935	128 (R)	256 (R)	>256 (R)	2 (S)	1 (S)	8 (R)	8 (R)	0.125 (S)	2 (S)	4	256	>2048

^aIMP = imipenem, MEM = meropenem, CAZ = ceftazidime, GEN = gentamicin, TOB = tobramycin, LEV = levofloxacin, CIP = ciprofloxacin, COL = colistin, TGC = tigecycline.
^bMinimum inhibitory concentrations classed as resistant (R) or sensitive (S).
^cCHG, chlorhexidine; p-CP, p-Chlorophenol; Ca(OCl)₂, calcium hypochlorite.

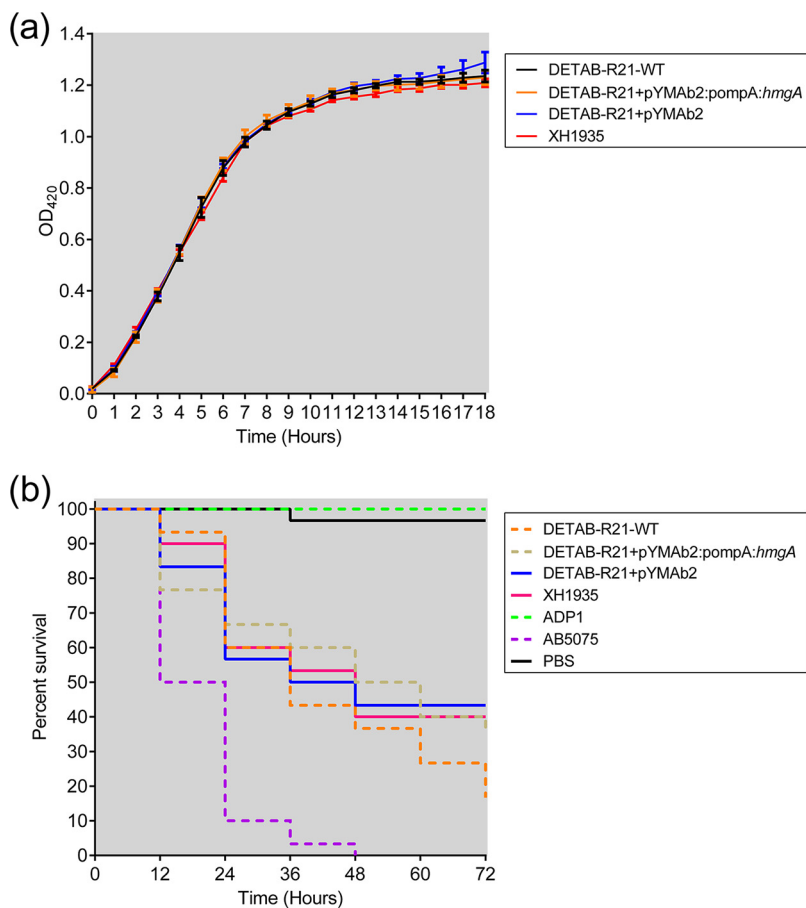


FIG 4 Growth curve and Kaplan-Meier survival curve. (a) cultures were incubated at 37°C with shaking and absorbance (OD420) were taken at the indicated time intervals. (b) Kaplan-Meier survival curve showing the virulence of different strains in *G. mellonella*. *G. mellonella* larvae ($n = 30$) were inoculated with 10^6 CFU. Survival was recorded per 12 h for 3 days.

OXA-23 and NDM-1 are relatively rare, especially when embedded within the chromosome and not on plasmids. Moreover, many studies found that NDM-1-positive CRAB are ST85_{Pas} from the Middle East (2). Miltgen et al. described an outbreak of OXA-23 and NDM-1 positive ST1_{Pas} *A. baumannii* without special phenotype in the Southwest Indian Ocean Area of France

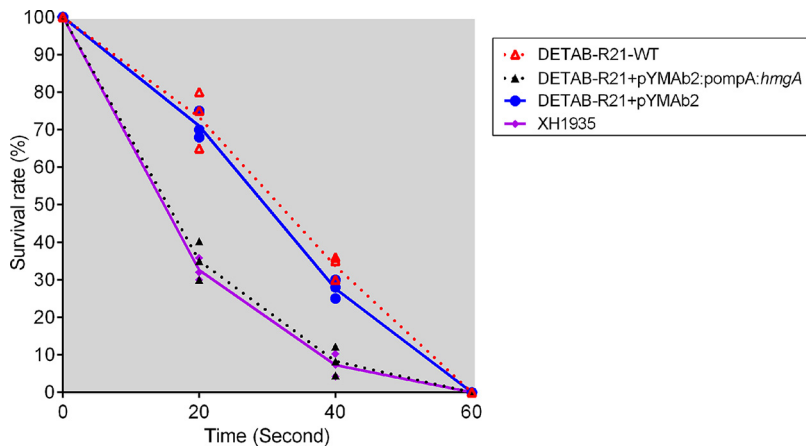


FIG 5 Bacterial survival rates under UV irradiation. Survival of DETAB-R21-WT, DETAB-R21+pYMAb2:pompA:hmgA, DETAB-R21+pYMAb2 and XH1935 after UV irradiation at 20 S, 40 S and 60 S, respectively. Survival was shown as data points.

(17). To our knowledge, our study is the first report of a ST164_{pas} *A. baumannii* strain, producing pyomelanin, in which OXA-23 and NDM-1 occur at the same time.

The OCL and KL gene clusters, which are responsible for biosynthesis of outer core of lipooligosaccharide and capsule, are potentially useful epidemiological markers (18). A study from Kenyon et al. in Australia reported in 82 GC1 and GC2 *A. baumannii* strains mainly contain OCL1 and OCL3 (19). Another report described from Wyres et al. revealed that among 3029 *A. baumannii* genomes, the most common OCL types were OCL1 (2086, 68.87%) and OCL3 (272, 8.98 %) (18). Typing cell-surface polysaccharide-determining regions of the DETAB-R21 chromosome revealed that it contains the relatively rare OCL5. Bioinformatic analyses from other researchers identified the most common KL types to be KL2 (713 of 2948 genomes, 24.2%) (18), followed by KL9 (343, 11.6%). DETAB-R21 again carries a less common type, the KL47 type.

Previous study found recombinase proteins XerC and XerD were responsible for resistance gene transfers via dif modules in plasmids, including carbapenemase genes *bla*_{OXA-24r} (20) *bla*_{OXA-58} (21) and tetracycline resistance gene *tet*(39) (22). However, we were unable to observe their function of all XerC/XerD and XerD/XerC sites for the mobile of the resistance genes. Conversely, transposons play an important role in the dissemination of carbapenemase genes *bla*_{OXA-23} and *bla*_{NDM-1} in this study. Our previous research found the standard Tn125 structure in a transferrable MDR plasmid in *A. baumannii* DETAB-P2 collected from the same ICU (21). A Tn125-like structure was also identified in this strain. Considering different TSD signature, we infer there are two possible reasons leading to the observed kind of Tn125-like structure formation. One possibility is mediated by two copies of IS*Aba125*, which differ from our previous report of Tn125 (21). Another possibility is that *bla*_{NDM-1} was flanked by two copies of IS*Aba14* which then inserted into the bacterial chromosome. According to the Tn125-like structure analysis in *A. baumannii* DETAB-R21, it may have evolved from the *A. baumannii* isolate TP2 found in the USA in 2016 or from the *A. baumannii* strain ACN21 collected in India in 2018. While we previously identified prophages containing the resistance gene in *A. baumannii* strains (12), Thomas et al. also reported the possibility of the *bla*_{NDM-1} transfer by a prophage (23). In this study, three prophage regions were identified in the chromosome of strain DETAB-R21. However, whether these prophage regions are able to form phage particles able to transfer the resistance genes remains to be confirmed.

Another interesting finding is that a composite transposon Tn2006 encoding the *bla*_{OXA-23} gene inserted into the chromosome and disrupted the *hmgA* gene, possibly leading to the production of dark brown pyomelanin. Our experimental data of *hmgA* overexpression strain construction established for the first time, that the *hmgA* gene plays a pivotal role in pyomelanin production. The impact of pyomelanin on phenotype in *A. baumannii* was further investigated. Certain virulence factors were identified in *A. baumannii*; Fonseca et al. considered that there might be a connection between pyomelanin production and virulence (10). However, in our study we tested virulence in the *G. mellonella* infection model, where we did not observe any difference in virulence whether or not the *A. baumannii* strains were producing pyomelanin. In addition, radiation resistance was observed in the pyomelanin-producing strain, meaning that the pigment may offer a potential protection effect for bacteria under UV. This could be of importance as UV sterilization is common but might be less effective in pigment producing strains.

Some limitations in this study remains, including the lack of knowledge of the biological functions of the dark brown pyomelanin. In addition, a murine infection model could be established to further evaluate the virulence level. Finally, either mechanism (natural transformation, conjugation, or phage transduction) of horizontal gene transfer (HGT) could transfer the Tn2006 and Tn125-like composite transposons need further explored (24–26).

Conclusions. This study describes and confirms the function of the gene *hmgA* for the tyrosine metabolic pathway in a pyomelanin-producing CRAB, the first time. Medically more relevant is the description of the resistance genes in the strain, with three copies of OXA-23 and one copy of NDM-1 inserted into the chromosome via different composite transposons, demonstrating the strong plasticity of the genome in *A. baumannii*. Due to increasing numbers of highly resistant strains which show resistance to a plethora of antibiotics, effective

monitoring and epidemic interventions should be implemented to decrease the dissemination of CRAB strains. If more pyomelanin-producing strains emerge, such as the one described in this study, this be a reason be concerned as the pigment may play a possible role in UV resistance.

MATERIALS AND METHODS

Ethics. Ethical approval and informed consent were obtained from the Sir Run Run Shaw Hospital (SRRSH) local ethics committee, Zhejiang University (approval number 20190802-1).

Patient information, bacterial isolation, medium, and culture condition. One 83-year-old female patient was admitted with severe pancreatitis in the ICU of SRRSH, Hangzhou, China in 11.12.2020. The patient was treated with 3.0 g meropenem per day for 6 days and underwent screening every week. DETAB-R21 was collected from the oral swab in 19.01.2021. Specifically, the swab was put into 2 mL TSB with 0.1% sodium thiosulfate and incubated at 37°C for 24 h. 20 μ L overnight culture was plated onto CHROMagar *Acinetobacter* sp. plates (CHROMagar, Paris, France) supplemented with 2 mg/L meropenem. After 24 h static incubation at 37°C, a single colony of presumptive *A. baumannii* was selected based on color and morphology, streaked onto a Mueller-Hinton (MH) agar plate (Oxoid, Hampshire, UK) and incubated overnight at 37°C. A single, isolated colony from the MH plate was selected and species were confirmed by MALDI-TOF MS (bioMérieux, Marcy-l'Étoile, France) and 16S rRNA gene sequencing. XH1935 was isolated from the sputum collected from another patient in the same ICU in 14.01.2021. The specific bacterial strains used in this study are listed in Table S1. The liquid medium used was MH broth (Oxoid, Hampshire, UK), which was supplemented with 100 hygromycin mg/L, as required.

Whole-genome sequencing and sequence analysis. Genomic DNA was extracted from *A. baumannii* DETAB-R21 and XH1935 using a Qiagen minikit (Qiagen, Hilden, Germany). Whole-genome sequencing was performed using both the Illumina HiSeq (Illumina, San Diego, USA) and the MinION (Nanopore, Oxford, UK) platforms (Weishu, Zhejiang, China). Assembly of the Illumina and Nanopore reads was performed using Unicycler v0.4.8 (27). Sequences were annotated using Prokka 1.14.0 (28). Multilocus sequence typing (MLST) with the Pasteur (29) and Oxford (30) schemes was performed via PubMLST (<https://pubmlst.org/>). Antimicrobial resistance genes were identified using ABRicate v0.8.13 (<https://github.com/tseemann/abricate>) with the ResFinder database (31) and insertion sequences were identified using ISFinder (32). Capsular polysaccharide (K locus) and lipooligosaccharide (OC locus) were tested using Bautype (33) and *Kaptive* (18), respectively. XerC/XerD and XerD/XerC recombinases recognition sites were detected using *pdiffinder* (<http://bacant.net/pdiff/>). The number of Single Nucleotide Polymorphisms (SNPs) in *A. baumannii* DETAB-R21 and XH1935 were calculated using Snippy v4.4.5 (<https://github.com/tseemann/snippy>) and snp-dists v0.6.3 (<https://github.com/tseemann/snp-dists>) (34). In addition, the PHAge Search Tool (PHASTER) was used for the prediction of bacteriophages (35).

Construction of *hmgA* overexpression strain. A complete fragment of *hmgA* was amplified from the *A. baumannii* strain XH1935. In addition, a strong promoter (from *pompA*) was also amplified from *A. baumannii* ATCC 17978. Primers are shown in Table S2. The products flanked by the recombination sequences were purified and cloned into the BamHI and Sall-digested shuttle plasmid vector pYMAb2-Hyg^r to yield the pYMAb2: *pompA:hmgA* using the ClonExpress II One Step Cloning kit (Vazyme Biotech Co., Ltd., Nanjing, China) according to the manufacturer's recommendations. pYMAb2: *pompA:hmgA* was then introduced into *A. baumannii* DETAB-R21 wild type (DETAB-R21-WT) by electroporation. pYMAb2-Hyg^r vector alone was also transformed into DETAB-R21-WT as a empty control to yield DETAB-R21 + pYMAb2.

Antimicrobial and disinfectant agents susceptibility testing. MICs for imipenem, meropenem, ceftazidime, gentamicin, tobramycin, ciprofloxacin, levofloxacin, colistin and tigecycline were determined using broth microdilution, with results interpreted using the CLSI 2021 guidelines. *Escherichia coli* ATCC 25922 served as the quality control strain. Moreover, MICs for disinfectants commonly used in the clinic setting, including chlorhexidine, p-Chlorophenol and calcium hypochlorite, were also measured using the broth microdilution method.

Growth curve measurement. Strains were streaked onto MH agar plates and incubated overnight at 37°C. Four independent cultures for every strain were grown overnight, diluted 1:1000 in MH broth and added into a flat-bottom honeycomb 100-well plate (Saue vald, Estonia) in three replicates. The plate was incubated at 37°C with agitation. Each culture was determined every 5 min for 18 h using a Bioscreen C MBR machine (Oy Growth Curves Ab Ltd., Finland) at a lower wide wavelength 420 nm as previous reports (36). Results were shown as OD₄₂₀ value per hour with triplicate independent replications.

***Galleria mellonella* infection model.** To compare the pathogenicity difference between pyomelanin and no pyomelanin producing strains, *Galleria mellonella* infection model was used as previously described (37, 38). Briefly, log-phase bacteria were centrifuged and resuspended in phosphate-buffered saline (PBS, Senrui, China) and underwent 10-fold serial dilutions to 1×10^6 CFU/mL. Ten μ L volume was injected into *G. mellonella* larvae ($n = 10$, 0.2 to 0.3 g; Yuejiayin, Tianjin, China) using Hamilton syringe (Hamilton, USA). *G. mellonella* larvae were incubated at 37°C in the dark and survival was recorded every 12 h and monitored for 3 days. *A. baumannii* AB5075 was used as a virulence positive control, *Acinetobacter baylyi* ADP1 served as a nonpathogenic negative control. Experiments were conducted in triplicate.

UV irradiation assay. UV irradiation assay was carried out based on the description of Thoms and Wackernagel with minor modification (39). The UVC irradiation could damage or destruct the DNA/RNA in various microbes (e.g., bacteria, fungi, and viruses) (40, 41). Overnight cultures in LB broth were centrifuged and resuspended in PBS (Senrui, China) with a final density of 10^8 cells/mL. Cells were irradiated under a UV lamp (Dose range: 0-6000 J/m², Wavelength: 254 nm, Wattage: 30 W, G30T8 UV UVC, Osram, USA) with the 60 cm distance at 20, 40 and 60 s, respectively. The depth of cell suspension was < 1 mm.

Cells was withdrawn and plated on MH agar plates after dilution for culture and further to calculate the bacterial survival rate with or without irradiation. Experiments were performed in triplicate.

Statistical analysis. *G. mellonella* survival rates were evaluated using Kaplan–Meier survival curves. Statistical significance was analyzed with a log-rank (Mantel–Cox) test using GraphPad Prism 8.0.2 (GraphPad Software, San Diego California USA). *P* values of < 0.05 was considered statistically significant.

Data availability. The complete sequences of the chromosome and five plasmids from *A. baumannii* DETAB-R21 have been deposited in the National Center for Biotechnology Information under BioProject [PRJNA716893](https://www.ncbi.nlm.nih.gov/bioproject/PRJNA716893), BioSample [SAMN23553142](https://www.ncbi.nlm.nih.gov/biosample/SAMN23553142), genome accession numbers [CP088895](https://www.ncbi.nlm.nih.gov/assembly/CP088895)–[CP088900](https://www.ncbi.nlm.nih.gov/assembly/CP088900). The *A. baumannii* XH1935 chromosomal sequence was deposited under BioProject [PRJNA716893](https://www.ncbi.nlm.nih.gov/bioproject/PRJNA716893), BioSample [SAMN23553143](https://www.ncbi.nlm.nih.gov/biosample/SAMN23553143), genome accession number [CP088894](https://www.ncbi.nlm.nih.gov/assembly/CP088894).

SUPPLEMENTAL MATERIAL

Supplemental material is available online only.

SUPPLEMENTAL FILE 1, PDF file, 0.5 MB.

ACKNOWLEDGMENTS

This work was undertaken with the support of National Key Research and Development Program of China grant (2018YFE0102100) and National Natural Science Foundation of China (81861138054, 82072313, 82072344).

We thank Te-Li Chen (National Yang-Ming University) for providing the plasmid pYMAb2. We appreciate Howard Shuman from the University of Chicago for kindly providing the *A. baumannii* pathogenic strain AB5075.

We have no conflicts of interest to declare.

REFERENCES

- Garnacho-Montero J, Dimopoulos G, Poulakou G, Akova M, Cisneros JM, De Waele J, Petrosillo N, Seifert H, Timsit JF, Vila J, Zahar JR, Bassetti M, European Society of Intensive Care M. 2015. Task force on management and prevention of Acinetobacter baumannii infections in the ICU. *Intensive Care Med* 41:2057–2075. <https://doi.org/10.1007/s00134-015-4079-4>.
- Zafer MM, Hussein AFA, Al-Agamy MH, Radwan HH, Hamed SM. 2021. Genomic characterization of extensively drug-resistant NDM-producing Acinetobacter baumannii clinical isolates with the emergence of novel bla ADC-257. *Front Microbiol* 12:736982. <https://doi.org/10.3389/fmicb.2021.736982>.
- Ruan Z, Chen Y, Jiang Y, Zhou H, Zhou Z, Fu Y, Wang H, Wang Y, Yu Y. 2013. Wide distribution of CC92 carbapenem-resistant and OXA-23-producing Acinetobacter baumannii in multiple provinces of China. *Int J Antimicrob Agents* 42:322–328. <https://doi.org/10.1016/j.ijantimicag.2013.06.019>.
- Di Venanzio G, Flores-Mireles AL, Calix JJ, Haurat MF, Scott NE, Palmer LD, Potter RF, Hibbing ME, Friedman L, Wang B, Dantas G, Skaar EP, Hultgren SJ, Feldman MF. 2019. Urinary tract colonization is enhanced by a plasmid that regulates uropathogenic Acinetobacter baumannii chromosomal genes. *Nat Commun* 10:2763. <https://doi.org/10.1038/s41467-019-10706-y>.
- Hamidian M, Nigro SJ. 2019. Emergence, molecular mechanisms and global spread of carbapenem-resistant Acinetobacter baumannii. *Microb Genom* 5.
- Hsu LY, Apisarnthanarak A, Khan E, Suwatarat N, Ghafur A, Tambyah PA. 2017. Carbapenem-resistant Acinetobacter baumannii and Enterobacteriaceae in South and Southeast Asia. *Clin Microbiol Rev* 30:1–22. <https://doi.org/10.1128/CMR.masthead.30-1>.
- Liu LL, Ji SJ, Ruan Z, Fu Y, Fu YQ, Wang YF, Yu YS. 2015. Dissemination of blaOXA-23 in Acinetobacter spp. in China: main roles of conjugative plasmid pAZJ221 and transposon Tn2009. *Antimicrob Agents Chemother* 59:1998–2005. <https://doi.org/10.1128/AAC.04574-14>.
- Wang Z, Li H, Zhang J, Wang H. 2021. Co-occurrence of blaOXA-23 in the chromosome and plasmid: increased fitness in carbapenem-resistant Acinetobacter baumannii. *Antibiotics (Basel)* 10:1196. <https://doi.org/10.3390/antibiotics10101196>.
- Bontron S, Nordmann P, Poirel L. 2016. Transposition of Tn125 encoding the NDM-1 carbapenemase in Acinetobacter baumannii. *Antimicrob Agents Chemother* 60:7245–7251. <https://doi.org/10.1128/AAC.01755-16>.
- Fonseca E, Freitas F, Caldart R, Morgado S, Vicente AC. 2020. Pyomelanin biosynthetic pathway in pigment-producer strains from the pandemic Acinetobacter baumannii IC-5. *Mem Inst Oswaldo Cruz* 115:e200371. <https://doi.org/10.1590/0074-02760200371>.
- Coelho-Souza T, Martins N, Maia F, Frases S, Bonelli RR, Riley LW, Moreira BM. 2014. Pyomelanin production: a rare phenotype in Acinetobacter baumannii. *J Med Microbiol* 63:152–154. <https://doi.org/10.1099/jmm.0.064089-0>.
- Loh B, Chen J, Manohar P, Yu Y, Hua X, Leptihn S. 2020. A biological inventory of prophages in *A. baumannii* genomes reveal distinct distributions in classes, length, and genomic positions. *Front Microbiol* 11:579802. <https://doi.org/10.3389/fmicb.2020.579802>.
- Nigro SJ, Brown MH, Hall RM. 2019. AbGR1-5, a novel AbGR1 variant in an Acinetobacter baumannii GC2 isolate from Adelaide, Australia. *J Antimicrob Chemother* 74:821–823. <https://doi.org/10.1093/jac/dky459>.
- Fernandez-Cuenca F, Tomas M, Caballero-Moyano FJ, Bou G, Pascual A, Spanish Society of Clinical M, Infectious D, Spanish Society of Clinical Microbiology and Infectious Diseases (SEIMC). 2018. Reporting antimicrobial susceptibilities and resistance phenotypes in Acinetobacter spp: a nationwide proficiency study. *J Antimicrob Chemother* 73:692–697. <https://doi.org/10.1093/jac/dkx464>.
- Boral B, Unaldi O, Ergin A, Durmaz R, Eser OK, Acinetobacter Study G. 2019. A prospective multicenter study on the evaluation of antimicrobial resistance and molecular epidemiology of multidrug-resistant Acinetobacter baumannii infections in intensive care units with clinical and environmental features. *Ann Clin Microbiol Antimicrob* 18:19. <https://doi.org/10.1186/s12941-019-0319-8>.
- Mentasti M, Prime K, Sands K, Khan S, Wootton M. 2020. Rapid detection of OXA-23-like, OXA-24-like, and OXA-58-like carbapenemases from Acinetobacter species by real-time PCR. *J Hosp Infect* 105:741–746. <https://doi.org/10.1016/j.jhin.2020.06.015>.
- Miltgen G, Bour M, Allyn J, Allou N, Vedani T, Vuilleminot JB, Triponney P, Martinet O, Lugagne N, Benoit-Cattin T, Dortet L, Birer A, Jaffar-Bandjee MC, Belmonte O, Plesiat P, Potron A. 2021. Molecular and epidemiological investigation of a colistin-resistant OXA-23-/NDM-1-producing Acinetobacter baumannii outbreak in the Southwest Indian Ocean area. *Int J Antimicrob Agents* 58:106402. <https://doi.org/10.1016/j.ijantimicag.2021.106402>.
- Wyres KL, Cahill SM, Holt KE, Hall RM, Kenyon JJ. 2020. Identification of Acinetobacter baumannii loci for capsular polysaccharide (KL) and lipooligosaccharide outer core (OCL) synthesis in genome assemblies using curated reference databases compatible with Kaptive. *Microb Genom* 6.
- Kenyon JJ, Holt KE, Pickard D, Dougan G, Hall RM. 2014. Insertions in the OCL1 locus of Acinetobacter baumannii lead to shortened lipooligosaccharides. *Res Microbiol* 165:472–475. <https://doi.org/10.1016/j.resmic.2014.05.034>.
- D'Andrea MM, Giani T, D'Arezzo S, Capone A, Petrosillo N, Visca P, Luzzaro F, Rossolini GM. 2009. Characterization of pABVA01, a plasmid encoding the OXA-24 carbapenemase from Italian isolates of Acinetobacter baumannii. *Antimicrob Agents Chemother* 53:3528–3533. <https://doi.org/10.1128/AAC.00178-09>.
- Liu H, Moran RA, Chen Y, Doughty EL, Hua X, Jiang Y, Xu Q, Zhang L, Blair JMA, McNally A, van Schaik W, Yu Y. 2021. Transferable Acinetobacter baumannii

- plasmid pDETAB2 encodes OXA-58 and NDM-1 and represents a new class of antibiotic resistance plasmids. *J Antimicrob Chemother* 76:1130–1134. <https://doi.org/10.1093/jac/dkab005>.
22. Blackwell GA, Hall RM. 2017. The tet39 determinant and the msrE-mpHE genes in *Acinetobacter* plasmids are each part of discrete modules flanked by inversely oriented pdfif (XerC-XerD) sites. *Antimicrob Agents Chemother* 61. <https://doi.org/10.1128/AAC.00780-17>.
 23. Krahn T, Wibberg D, Maus I, Winkler A, Bontron S, Sczyrba A, Nordmann P, Puhler A, Poirel L, Schluter A. 2016. Intraspecies transfer of the chromosomal *Acinetobacter baumannii* blaNDM-1 carbapenemase gene. *Antimicrob Agents Chemother* 60:3032–3040. <https://doi.org/10.1128/AAC.00124-16>.
 24. Hamidian M, Hawkey J, Wick R, Holt KE, Hall RM. 2019. Evolution of a clade of *Acinetobacter baumannii* global clone 1, lineage 1 via acquisition of carbapenem- and aminoglycoside-resistance genes and dispersion of ISAb1. *Microb Genom* 5.
 25. Holt K, Kenyon JJ, Hamidian M, Schultz MB, Pickard DJ, Dougan G, Hall R. 2016. Five decades of genome evolution in the globally distributed, extensively antibiotic-resistant *Acinetobacter baumannii* global clone 1. *Microb Genom* 2:e000052. <https://doi.org/10.1099/mgen.0.000052>.
 26. Godeux AS, Svedholm E, Barreto S, Potron A, Venner S, Charpentier X, Laaberk MH. 2022. Interbacterial transfer of carbapenem resistance and large antibiotic resistance islands by natural transformation in pathogenic *Acinetobacter*. *mBio* 13:e0263121. <https://doi.org/10.1128/mbio.02631-21>.
 27. Wick RR, Judd LM, Gorrie CL, Holt KE. 2017. Unicycler: resolving bacterial genome assemblies from short and long sequencing reads. *PLoS Comput Biol* 13:e1005595. <https://doi.org/10.1371/journal.pcbi.1005595>.
 28. Seemann T. 2014. Prokka: rapid prokaryotic genome annotation. *Bioinformatics* 30:2068–2069. <https://doi.org/10.1093/bioinformatics/btu153>.
 29. Diancourt L, Passet V, Nemeč A, Dijkshoorn L, Brisse S. 2010. The population structure of *Acinetobacter baumannii*: expanding multiresistant clones from an ancestral susceptible genetic pool. *PLoS One* 5:e10034. <https://doi.org/10.1371/journal.pone.0010034>.
 30. Bartual SG, Seifert H, Hippler C, Luzon MA, Wisplinghoff H, Rodriguez-Valera F. 2005. Development of a multilocus sequence typing scheme for characterization of clinical isolates of *Acinetobacter baumannii*. *J Clin Microbiol* 43:4382–4390. <https://doi.org/10.1128/JCM.43.9.4382-4390.2005>.
 31. Zankari E, Hasman H, Cosentino S, Vestergaard M, Rasmussen S, Lund O, Aarestrup FM, Larsen MV. 2012. Identification of acquired antimicrobial resistance genes. *J Antimicrob Chemother* 67:2640–2644. <https://doi.org/10.1093/jac/dks261>.
 32. Siguier P, Perochon J, Lestrade L, Mahillon J, Chandler M. 2006. ISfinder: the reference centre for bacterial insertion sequences. *Nucleic Acids Res* 34:D32–D36. <https://doi.org/10.1093/nar/gkj014>.
 33. Yu H, Lu S, Gasior K, Singh D, Vazquez-Sanchez S, Tapia O, Toprani D, Beccari MS, Yates JR, 3rd, Da Cruz S, Newby JM, Lafarga M, Gladfelter AS, Villa E, Cleveland DW. 2021. HSP70 chaperones RNA-free TDP-43 into anisotropic intranuclear liquid spherical shells. *Science* 371. <https://doi.org/10.1126/science.abb4309>.
 34. Bush SJ. 2021. Generalizable characteristics of false-positive bacterial variant calls. *Microb Genom* 7.
 35. Zhou Y, Liang Y, Lynch KH, Dennis JJ, Wishart DS. 2011. PHAST: a fast phage search tool. *Nucleic Acids Res* 39:W347–W352. <https://doi.org/10.1093/nar/gkr485>.
 36. Zeng Z, Guo XP, Cai X, Wang P, Li B, Yang JL, Wang X. 2017. Pyomelanin from *Pseudoalteromonas lipolytica* reduces biofouling. *Microb Biotechnol* 10:1718–1731. <https://doi.org/10.1111/1751-7915.12773>.
 37. Xu Q, Chen T, Yan B, Zhang L, Pi B, Yang Y, Zhang L, Zhou Z, Ji S, Leptihn S, Akova M, Yu Y, Hua X. 2019. Dual role of gnaA in antibiotic resistance and virulence in *Acinetobacter baumannii*. *Antimicrob Agents Chemother* 63. <https://doi.org/10.1128/AAC.00694-19>.
 38. Wagley S, Borne R, Harrison J, Baker-Austin C, Ottaviani D, Leoni F, Vuddhakul V, Titball RW. 2018. *Galleria mellonella* as an infection model to investigate virulence of *Vibrio parahaemolyticus*. *Virulence* 9:197–207. <https://doi.org/10.1080/21505594.2017.1384895>.
 39. Thoms B, Wackernagel W. 1982. UV-induced alleviation of lambda restriction in *Escherichia coli* K-12: kinetics of induction and specificity of this SOS function. *Mol Gen Genet* 186:111–117. <https://doi.org/10.1007/BF00422921>.
 40. Bhardwaj SK, Singh H, Deep A, Khatri M, Bhaumik J, Kim KH, Bhardwaj N. 2021. UVC-based photoinactivation as an efficient tool to control the transmission of coronaviruses. *Sci Total Environ* 792:148548. <https://doi.org/10.1016/j.scitotenv.2021.148548>.
 41. Smolle C, Huss F, Lindblad M, Reischies F, Tano E. 2018. Effectiveness of automated ultraviolet-C light for decontamination of textiles inoculated with *Enterococcus faecium*. *J Hosp Infect* 98:102–104. <https://doi.org/10.1016/j.jhin.2017.07.034>.